

Time-Domain Traveling-Wave Model of Distributed-feedback Quantum Cascade Laser

Sara Zaminga*, Lorenzo Columbo†, Carlo Silvestri ‡, Mariangela Gioannini†, and Frédéric Grillot*

*LTCI Télécom Paris, Institut Polytechnique de Paris, Palaiseau, France

†Dipartimento di Elettronica e Telecomunicazioni, Politecnico di Torino, Torino, Italy

‡School of Information Technology and Electrical Engineering, The University of Queensland, Brisbane, Australia

Email: sara.zaminga@telecom-paris.fr

Abstract—In this paper, a time-domain (TD) traveling-wave (TW) model based on the Effective Semiconductor Maxwell-Bloch Equations (ESMBEs) and a coupled-mode theory is proposed for the description of the dynamics of a mid-Infrared (mid-IR) Quantum Cascade Laser (QCL) in the Distributed-Feedback (DFB) configuration. The influence of physical and geometrical properties on the QCL's dynamics is investigated. Numerical simulations find good agreement with the experimental results obtained with a DFB QCL operating at 9.34 μm .

Index Terms—Quantum cascade laser, distributed-feedback laser, time-domain traveling-wave model, coupled-mode theory

I. INTRODUCTION

The Quantum Cascade Laser (QCL) is an outright semiconductor technology, based on unipolar intersubband transitions for light generation [1]. Thanks to their engineered superlattice heterostructure, these stable and compact sources are widely tunable across the infrared spectrum. Thus, being compliant with multiple applications, i.e. free-space communications [2] and precision spectroscopy [3], they are nowadays massively exploited. Yet, manifold aspects regarding their dynamics are to be inspected on a theoretical viewpoint. The most extensively encountered model in literature relies on semiclassical rate equations [4]. A valid alternative treats the QCL as a classic atomic-like two or three-level system through Maxwell-Bloch Equations (MBEs) [5]. MBEs do not encompass the presence of the linewidth enhancement factor (LEF) and the associated asymmetric gain and refractive index profiles, unlike the Effective Semiconductor Maxwell-Bloch Equations (ESMBEs), proposed in [6] for the Fabry-Perot (FP) configuration and in [7] for the innovative ring configuration. This paper introduces a novel extension to the existing model in [6] by integrating the impact of distributed-feedback (DFB) through the application of coupled-mode theory [8]. By employing this rigorous approach, we achieve a comprehensive investigation of the mechanism responsible for single-mode selection in DFB QCLs. Remarkably, to the best of our knowledge, this work represents the first implementation of such an extension, signifying an important advancement in the field.

II. NUMERICAL MODEL AND SIMULATIONS

With respect to the model detailed in [6], the forward and backward electric fields F , R satisfy the approximated coupled

equation 1, where $\kappa \triangleq j\kappa_{DFB}e^{j\Phi}$, according to the theory in [8].

$$\frac{\partial}{\partial z} \begin{bmatrix} F(z, t) \\ R(z, t) \end{bmatrix} = \begin{bmatrix} 0 & -i\kappa \\ i\kappa^* & 0 \end{bmatrix} \begin{bmatrix} F(z, t) \\ R(z, t) \end{bmatrix} \quad (1)$$

where κ_{DFB} is the coupling coefficient of the grating, assumed to be real. To numerically solve the resulting TD-TW model, the split-step method (SS-TDM) proposed in [9] is applied.

The simulations criteria emerge from a trade-off between spectral resolution and CPU time for simulation. Table I reports the values of the parameters used in simulations. The model validation develops from the comparison between the FP and DFB configurations (see Figure 2a-b). As expected, in the latter case the laser is characterized by single-mode emission for a wider interval of bias current values, according to the physical and material properties, as explained hereafter. $\kappa_{DFB} = 7 \text{ cm}^{-1}$ is set to match the behavior of the QCL under study, expected to be $< 10 \text{ cm}^{-1}$ according to the vendor's information. The reflectivity of the front facet is 0.32, since it is cleaved in the QCL under test. The grating losses α_{DFB} and the internal efficiency η_i have been introduced in the model, to match the experimental threshold current and fit the slope of the Light-CI (LC) curve (see Figure 1a, differential efficiency $\eta_{d_{exp}} \approx \eta_{d_{sim}} \approx 0.3$). The agreement of the two curves is qualitatively good, apart from larger values of bias current, where they diverge because the thermal quenching is not included in the simulation model. Figures 1b-c represent the maps of respectively the experimental and simulation optical spectra. The former depicts a turning point from single- to multi-mode emission for bias currents above 380 mA. To simulate such dynamics, we set LEF=0.9 in the simulation. Despite the disparity in resolution and scale of the frequency axis between Figures 1d and its inset, attributable to a lower resolution and a reduced number of data points in the experimental trace, a remarkable agreement is observed between the two maps: when the laser operates multi-mode, the side-modes are separated by a consistent distance of around 22 GHz, corresponding to a cavity length $L=2 \text{ mm}$.

This research explores also the effect of the LEF on the single-mode emission of the QCL: arising from the carrier-induced refractive index change in semiconductor materials, this dimensionless quantity characterizes the nonlinear

TABLE I
MATERIAL AND DEVICE PARAMETERS USED IN SIMULATIONS FOR THE QCL IN THE DFB CONFIGURATION

| n | L (mm) | V (μm^3) | R_{front} | R_{back} | $\alpha_i + \alpha_{DFB}$ (cm^{-1}) | η_i | f_0 (μm^3) | τ_e (ps) | τ_d (ps) | λ_0 (μm) |
|-----|--------|-----------------------|-------------|------------|--|----------|---------------------------|---------------|---------------|-------------------------------|
| 3.3 | 2 | 2200 | 0.32 | 0.99 | 10 + 11.8 | 0.80 | 1.6×10^{-7} | 1.64 | 0.1 | 9.34 |

response of the laser's optical frequency. It influences the spectral purity, stability, and coherence of the laser output, affecting crucial parameters such as linewidth, chirp and modulation bandwidth. Our findings reveal an almost decreasing-exponential relation of the bias current value at which the laser switches from single-mode to multi-mode operation, when increasing the LEF value (see Figure 3a). The same study has been extended to κ_{DFB} , although without revealing a definite mathematical relation. Nonetheless, from Figure 3b, it is apparent that an optimal value of κ_{DFB} can be determined allowing for a wider range of bias currents that sustain single-mode emission. Notably, the impact of κ_{DFB} is more pronounced when the LEF value is lower. Finally, the deposition of an anti-reflection (AR) coating on the front facet increases the laser's threshold, but more importantly it grants a widening of the range of bias currents for which we observe the single-mode emission, as it is clearly displayed in Figure 2b-c.

III. CONCLUSION

In this paper, we adopted a new TD-TW model based on a set of ESMBEs and a coupled mode approach to simulate the dynamics of DFB QCLs. We managed to qualitatively reproduce experimental findings relative to a DFB QCL operating at 9.34 μm in continuous-wave and room-temperature conditions. We underline how the material and device properties are crucial for achieving optimal laser performance. Future studies will investigate other dynamical phenomena, i.e. the effect of external optical feedback and level of intensity and phase noise. Since the latter might have a substantial impact on niche applications of DFB QCLs, e.g. secure chaotic communications [10], a more rigorous theoretical treatment might furnish a deeper understanding and a more realistic interpretation of the experimental outcomes.

REFERENCES

- [1] Faist, J. et al., *Science* 264, 553-556 (1994).
- [2] Didier, P. et al., *Photonics Research* 11, 582-590 (2023).
- [3] Sterczewski, L., et al., *Optical Engineering* 57, 011014 (2018).
- [4] Page, H. et al., *Appl. Phys. Lett.* 78, 22: 3529-3531 (2001).
- [5] Gordon, A. et al., *Phys. Rev. A* 77, 053804 (2002).
- [6] Silvestri, C. et al., *Opt. Express* 28, 23846-23861 (2020).
- [7] Columbo, L. L. et al., *Opt. Express* 26, 2829-2847 (2018).
- [8] Tromborg, B. et al., *IEEE Journal of Quantum Electronics* 23, 11, 1875-1889 (1987).
- [9] Kim, B. et al., *IEEE Journal of Quant. Electr.* 36, 7, 787-794 (2000).
- [10] Spitz, O. et al., *Nat Commun* 12, 3327 (2021).

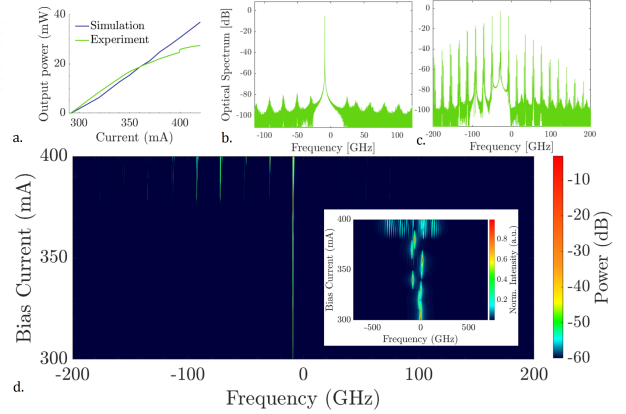


Fig. 1. (a) Comparison of Light-Current (LC) curve retrieved from simulations (blue) and experiments (green). (b) Optical spectrum for a bias of 330 mA (single-mode emission, side modes suppressed). (c) Optical spectrum for a bias of 400 mA (multi-mode emission). (d) Simulation and experimental (inset) optical spectra maps of the DFB QCL for a bias sweep of [300-400] mA. The quantity $f - f_0$ ($f_0 = \frac{c}{\lambda_0}$) is represented along x .

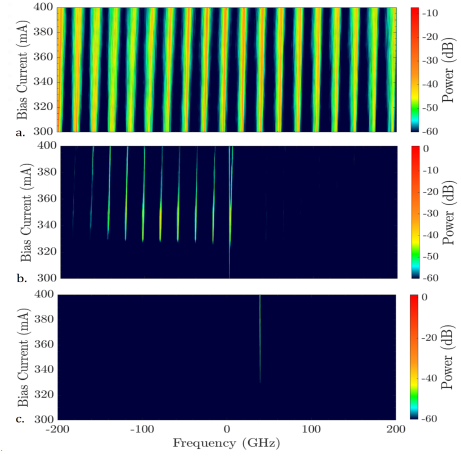


Fig. 2. Optical spectra maps for: FP (a), DFB with cleaved front facet (b), DFB with AR-coated front facet (c) configurations. The quantity $f - f_0$ ($f_0 = \frac{c}{\lambda_0}$) is represented along x .

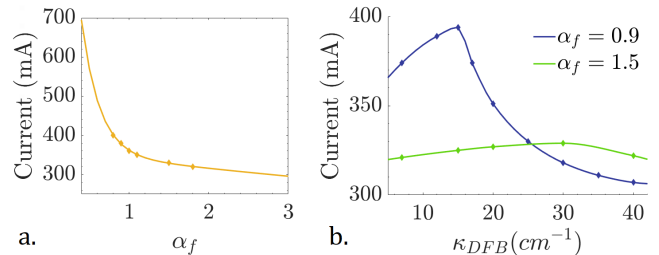


Fig. 3. Dependence on (a) LEF and (b) κ_{DFB} of the bias current range where single-mode emission is observed.